ARL-TR-8413 ● JULY 2018

US Army Research Laboratory

New Insight toward Dynamic Impedance Optimization in Glass/Polymer Composites: The Role of Segmental Dynamics of Interlayers

by Alex J Hsieh, David Veysset, Daniel F Miranda, Steven E Kooi, James Runt, and Keith A Nelson

NOTICES

Disclaimers

The findings in this report are not to be construed as an official Department of the Army position unless so designated by other authorized documents.

Citation of manufacturer's or trade names does not constitute an official endorsement or approval of the use thereof.

Destroy this report when it is no longer needed. Do not return it to the originator.

ARL-TR-8413 ● JULY 2017

US Army Research Laboratory

New Insight toward Dynamic Impedance Optimization in Glass/Polymer Composites: The Role of Segmental Dynamics of Interlayers

by Alex J Hsieh
Weapons and Materials Research Directorate, ARL

David Veysset and Keith A Nelson
Institute for Soldier Nanotechnologies, Massachusetts Institute of Technology, Cambridge, MA
Department of Chemistry, Massachusetts Institute of Technology, Cambridge, MA

Steven E Kooi
Institute for Soldier Nanotechnologies, Massachusetts Institute of Technology, Cambridge, MA

Daniel F Miranda and James Runt
Department of Materials Science and Engineering, Penn State University, University Park, PA

REPORT DOCUMENTATION PAGE

Form Approved
OMB No. 0704-0188

1. REPORT DATE *(DD-MM-YYYY)*	2. REPORT TYPE	3. DATES COVERED (From - To)
July 2018	Technical Report	1 January 2017–28 February 2018

4. TITLE AND SUBTITLE
New Insight toward Dynamic Impedance Optimization in Glass/Polymer Composites: The Role of Segmental Dynamics of Interlayers

5a. CONTRACT NUMBER

5b. GRANT NUMBER

5c. PROGRAM ELEMENT NUMBER

6. AUTHOR(S)
Alex J Hsieh, David Veysset, Daniel F Miranda, Steven E Kooi, James Runt, and Keith A Nelson

5d. PROJECT NUMBER

5e. TASK NUMBER

5f. WORK UNIT NUMBER

7. PERFORMING ORGANIZATION NAME(S) AND ADDRESS(ES)
US Army Research Laboratory
ATTN: RDRL-WMM-G
Aberdeen Proving Ground, MD 21005-5069

8. PERFORMING ORGANIZATION REPORT NUMBER
ARL-TR-8413

9. SPONSORING/MONITORING AGENCY NAME(S) AND ADDRESS(ES)

10. SPONSOR/MONITOR'S ACRONYM(S)

11. SPONSOR/MONITOR'S REPORT NUMBER(S)

12. DISTRIBUTION/AVAILABILITY STATEMENT
Approved for public release; distribution is unlimited.

13. SUPPLEMENTARY NOTES

14. ABSTRACT
Recent observations on the influence of high-rate deformation-induced glass transition affecting the dynamic impact response in poly(urethane urea) (PUU) elastomers has inspired a new inquiry into whether enabling molecular mechanisms could also benefit dynamic impedance optimization at the interface of a glass/polymer bilayer, particularly at the moment of target/impulse interaction. In this work, we investigated the molecular influence on dynamic stiffening and strengthening observed under microballistic measurements of two bulk elastomers—a PUU and a polyurea. Upon impact at strain rates of approximately 10^8/s, PUU exhibited a moderate improvement over polyurea in resistance against penetration that is more pronounced at higher speeds. The variation in dynamic stiffening corroborates well with the corresponding segmental dynamics data determined via broadband dielectric relaxation. Meanwhile, we calculated the shock impedance from the shock velocity data derived from the respective shock Hugoniot. Results strongly indicate the efficacy of dynamic impedance optimization between PUU and glass, which is greatly desired for mitigating reflective tensile stress waves and limiting the propensity of further fracture in the glass. New insight on molecular attributes of hierarchical elastomers will guide the glass/polymer interface designs for integration into advanced lightweight transparent armor with multihit performance capability.

15. SUBJECT TERMS
dynamic impedance, shock Hugoniot, segmental dynamics, poly(urethane urea), polyurethane, laminated glass/polymer composites, dynamic stiffening, high-rate deformation-induced glass transition, microballistic measurements

16. SECURITY CLASSIFICATION OF:			17. LIMITATION OF ABSTRACT	18. NUMBER OF PAGES	19a. NAME OF RESPONSIBLE PERSON
a. REPORT	b. ABSTRACT	c. THIS PAGE			Alex J Hsieh
Unclassified	Unclassified	Unclassified	UU	35	19b. TELEPHONE NUMBER (Include area code) (410) 306-2292

Contents

List of Figures

List of Tables

Acknowledgments

This report is based upon work supported in part by the US Army Research Laboratory (ARL) and the US Army Research Office through the Institute for Soldier Nanotechnologies under contract number W911NF-13-D-0001. Co-authors David Veysset and Keith A Nelson also acknowledge support through the Office of Naval Research (ONR), DURIP Grant No. N00014-13-1-0676. Co-authors Daniel F Miranda and James Runt gratefully acknowledge the support of ONR under grant N00014-14-C-0205. Lead author Alex J Hsieh would like to thank Dr Robert M Elder and Dr John J La Scala at ARL for fruitful discussions, and also acknowledge Dr Daniel T Casem at ARL for his assistance in the previously published plate impact measurements.

1. Introduction

Advancement in high-performance glass and polymeric materials has led to the development of lightweight hybrid composites for use in a broad range of ballistic protective material systems[1,2] such as windows and vision blocks for vehicles and rotorcraft. Glass has high hardness and is used as the strike face for providing stiffness, hardness, and durability, while the backing polymer layers serve to protect against spall. The impact response of laminated composite structures is known to be complex,[3] where multihit impact performance capability is desired particularly for the advanced lightweight hybrid systems.[4] Traditional designs of these materials are often based on stiffness and toughness; however, these standard bulk material attributes are neither sufficient to quantify how fast molecules in a polymer can change their mobility with respect to the rate of deformation nor the propensity toward a change of their respective physical state during dynamic deformation. Meanwhile, for laminated composite structures it was noted that incorporation of a high-wave-speed layer could lead to better dissipation of impulse energy as well as improve the overall impact performance.[3]

Over the last decade, nature has provided an inspiration toward the rational design of hybrid composites, where hierarchical architectures in structural biological materials such as shells and bones have been attributed to the robust mechanical strength characteristics that were deemed essential for protection against dynamic environmental threats.[5–9] One such concept of note is a gradient approach used in the design of graded composites, wherein incorporation of a bone-inspired hierarchy—a soft–stiff–soft–stiff material distribution pattern based on the bone-foramen and osteonal-bone material systems—demonstrated enhanced shock-wave mitigation capability.[8] Even so, neither nature nor prior experiments explicitly revealed the role of dynamics at the molecular level. Meanwhile, there is a lack of understanding of the underpinning molecular mechanisms and their influence on material deformation, particularly at the moment of impulse interaction. Such knowledge can provide insights toward manipulating the physics of failure for design of robust material systems.

Recently, Veysset et al. used a laser-induced microballistic impact platform and shown its capability of providing real-time multiframe imaging for in situ visualization and differentiation of material deformation at strain rates on the order of 10^8/s.[10–13] In particular, the resulting dynamic stiffening phenomenon during such high-velocity impact was first revealed in hierarchical poly(urethane urea) (PUU) elastomers, but not in a polydimethylsiloxane elastomer, when impacted by silica microparticles.[10] PUUs were noted to exhibit complex microstructure[14–17]

along with a broad range of relaxation times,[18,19] where the segmental mobility of the soft phase was shown to be strongly dependent upon the extent of intersegment mixing between soft and hard segments.[17–19] Among these PUUs, soft phases associated with greater phase-mixed regions revealed longer relaxation times on the order of microseconds at ambient conditions.[10,17] The presence of these slower dynamics components was found to be key to enabling dynamic stiffening, presumably via a high-rate deformation-induced glass transition mechanism,[11,17] while those with nanosecond relaxation times at ambient conditions were presumably capable of providing additional energy absorption toward dynamic strengthening.[10–11] Furthermore, it was also noted that for PUUs a cooperative molecular relaxation mechanism, facilitated by the presence of intermolecular hydrogen bonding throughout the physically crosslinked network, could be a plausible pathway toward both dynamic stiffening and dynamic strengthening.[11,17,19] In comparison, PUUs regardless of their respective composition exhibited greater dynamic stiffening during impact at strain rates on the order of 10^8/s than a glassy bisphenol A polycarbonate despite the high fracture toughness and ballistic strength of the latter.[11] Dynamic stiffening over the same impact velocity range was not evidenced for polycarbonate; instead, plastic deformation was the predominant mode of deformation, presumably due to the lack of a cooperative intermolecular hydrogen-bond relaxation mechanism and a microsecond relaxation.[11]

Our motivation for this study was to discern whether the high-rate dynamic stiffening phenomena observed in the bulk PUUs can serve as an effective energy dissipation pathway, including the potential of its influence toward shock-wave propagation during ballistic impact for interlayer materials that are used in bonding between the layers of laminated glass/polymer composites. Meanwhile, the shock Hugoniot is regarded as the most fundamental description of the thermodynamic state of a material following the passage of a shock wave.[20] Impedance, on the other hand, is a useful concept for better understanding of the flow of impact energy during the ballistic shock events,[21,22] where shock-wave impedance differing from the acoustic wave impedance is determined by the product of density and the shock velocity determined at a given impact velocity, hereafter called shock impedance. During rapid impulse loading, the stress wave, when it reaches the interface between glass and a polymer sublayer, could reflect as a tensile stress wave back to the glass layer due to the acoustic impedance mismatch between these two materials. Consequently, the resultant tensile stress waves could cause initiation of cracks from the back side of glass and propagate further into the glass, which would significantly limit the desired multihit performance capability. Polyurethane-based adhesives are often used in laminated glass/polymer composites, where a thicker

interlayer is preferred for use to bond between glass and a polymer layer than those used to bond between polymer layers (50 vs. 25 μm, respectively). This is a common practice for better accommodation of the mismatch in coefficients of thermal expansion between glass and polymer layers, as well as to prevent crack propagation from the front glass layers into the polycarbonate backing layers.[4]

In this report, we focus on the molecular influence of polymers where material deformation upon ballistic impact at a glass/polymer interface could be a strong function of their corresponding segmental dynamics. First, we exploit laser-induced microballistic measurements and compare the high strain-rate deformation response of a bulk PUU against impact by silica as well as steel microparticles, which are of higher impedance than silica microparticles. With respect to the role of segmental dynamics, we used broadband dielectric relaxation measurements to further discern and differentiate its influence on the extent of dynamic stiffening observed upon microballistic impact between PUU and a polyurea. In addition, we highlighted the essence of high-rate deformation-induced glass transition observed in a bulk PUU and determine its efficacy toward the overall dynamic impedance optimization at the interface between glass and polymer layers. This is elucidated through analysis of the extent of shock-wave reflection at the interface of each respective bilayer, which is calculated based on the corresponding shock Hugoniot data.

2. Experimental

The model elastomers chosen for microballistic impact studies and broadband dielectric relaxation spectroscopy measurements included PUU 532-1000 and polyurea 1000. The PUU 532-1000 was prepared via a two-step prepolymer synthesis,[23] which is composed of 4,4'-dicyclohexylmethane diisocyanate (HMDI), diethyltoluenediamine (DETA), and poly(tetramethylene oxide) (PTMO), with a molar ratio of 5:3:2 for [HMDI]:[DETA]:[PTMO], where the molecular weight of PTMO is 1000 g/mol. The polyurea 1000 was formed by reaction of poly(tetramethylene oxidedi-p-aminobenzoate) (Versalink P1000, Air Products) and a polycarbodiimidemodified diphenylmethane diisocyanate (Isonate 143 L, Dow Chemical) at a 4:1 weight ratio. The molecular weight given by the manufacturer for the PTMO-amine component is M = 1238 ± 72 g/mol. The nominal hard segment contents of both PUU 532-1000 and polyurea 1000 are very similar, approximately 34 wt%. More details on the synthesis of PUU and polyurea can be found in Sarva and Hsieh[23] and Choi et al.,[24] respectively, and on the characterization of these materials.[16–19, 24–26]

The high-strain-rate deformation response of selected elastomers was investigated by using a laser-induced microballistic impact test platform, as shown in Fig. 1.[10,27] The launching pad assembly consists of a 210-µm glass substrate, a 60-nm gold film for laser absorption, a 30-µm layer of cross-linked polyurea (different from the polyurea 1000), and a submonolayer of either silica microspheres (diameter D = 7.4 µm) or steel microspheres (D = 20 µm ± 2 µm) deposited on top of the assembly as described in Veysset et al.[10] Upon laser ablation of the gold film using a 10-ns duration, 532-nm wavelength laser pulse focused in a region of about 50-µm diameter, the polyurea layer expands and launches the particles into free space. The particle speed is adjusted from 100 to 800 m/s by varying the laser pulse energy from 2 to 60 mJ (Fig. 1). The projectiles are ejected into free space and impact a target sample at near-normal incidence (±5°). The launching pad and the target are separated by approximately 1.0 mm. Using a high-speed camera (SIMX16, Specialised Imaging), consisting of 16 charge-coupled devices, which are independently triggerable, with exposure times as short as 2 ns and variable interframe times, we visualized the microspheres as they impacted the surface of the samples and subsequently rebounded, providing insight into the high-strain-rate deformation response of these selected polymeric materials. Both impact and rebound velocities and maximum and residual (final) penetration depths were extracted from the 16-frame videos. The maximum depth of penetration (DOP) occurs in the first instants following impact; thereafter, the polymer fully responds to the impact and the DOP decreases. A more detailed description of the imaging setup and image analysis is available in Veysset et al.[10]

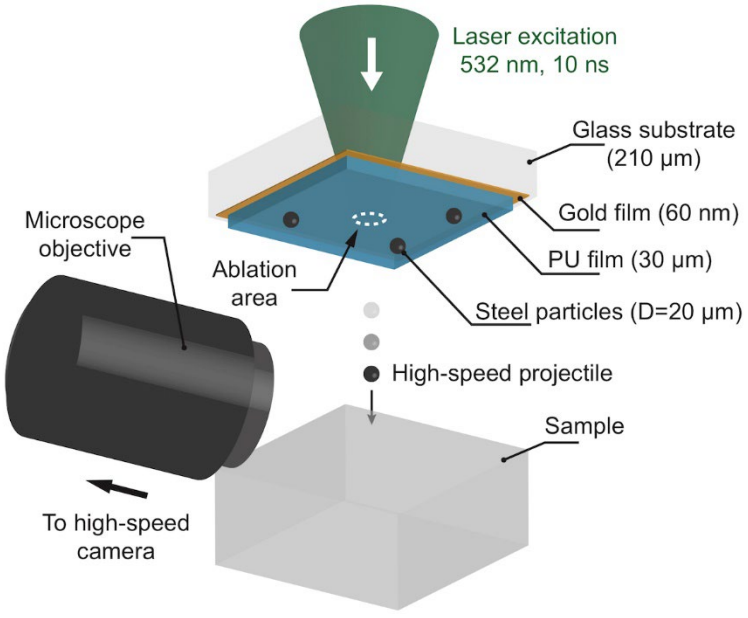

Fig. 1 Schematic of the laser-induced particle impact test

Dielectric relaxation spectroscopy measurements were carried out using a parallel plate geometry, where samples in the form of disks (15- to 20-mm diameter, 0.1−0.3 mm thick) were sandwiched between 20-mm-diameter brass electrodes to form a parallel plate capacitor. Isothermal relaxation spectra were collected for PUU 532-1000 and polyurea 1000 under a very dry nitrogen atmosphere as a function of temperature using a Novocontrol Concept 40 spectrometer from 0.01 to 10 MHz on heating from −150 to 200 °C.

3. Results

3.1 Microballistic Impact Response of PUU 532-1000 against Silica and Steel Micro Particles

As shown in Fig. 2, reproduced from Hsieh et al.,[28] the capability of direct visualization of the impact of microprojectiles on substrates and in situ characterization, including DOP and the extent of rebound of the microprojectiles, is clearly demonstrated. In Fig. 2a, representative impact sequences of PUU 532-1000 by silica microspheres of 7-μm diameter are shown, where rebound of a microparticle is evidenced during impact at 740 m/s, with the sample surface undergoing extreme deformation, at a strain rate on the order of 10^8 s^{-1}, to conform to the impacting spherical projectile. Meanwhile, we also carried out microballistic measurements with 20-μm steel particles to validate our findings on the dynamic stiffening and strengthening characteristics observed in PUUs upon impact by silica microparticles. Since the steel microprojectiles are larger and denser than the silica projectiles, it is expected that they would impart greater kinetic energy and momentum. In the case of impact by steel microparticles, rebound of steel microparticles still occurs when PUU 532-1000 was impacted at speeds below approximately 500 m/s. Figure 2b shows the representative impact sequences observed for PUU 532-1000, where rebound of a steel microparticle is evidenced during impact at 470 m/s speed. The steel microprojectile is noted to penetrate to a full diameter under the surface of PUU 532-1000, where the average normalized maximum DOP was found to be greater than those obtained upon impact by silica microparticles at much higher speeds.

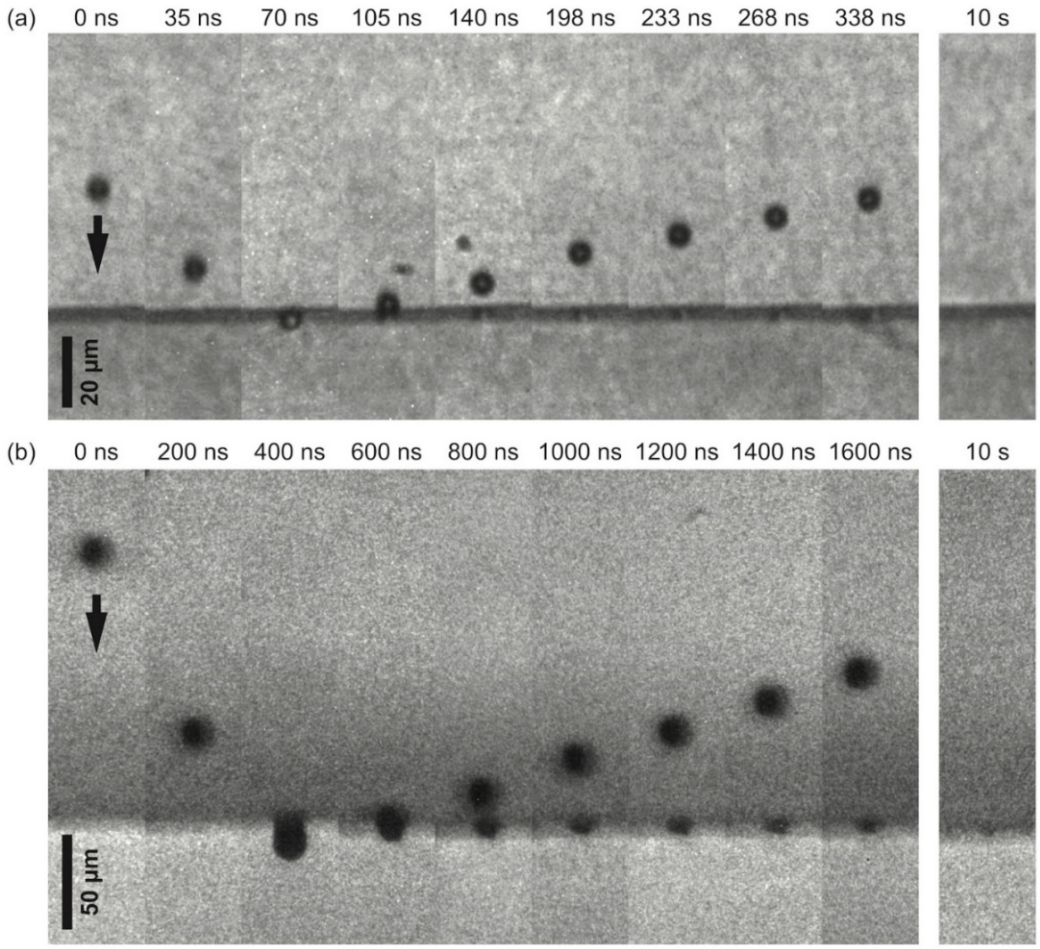

Fig. 2 Typical sequence of images recorded using a high-speed camera with 3-ns exposure time showing particle impact on a PUU 532-1000 sample (reproduced from Hsieh et al.[28]). a) 10 of 16 images of impact by 7.4-µm silica microparticle with a speed of 740 m/s and b) 9 of 16 images of impact by 20-µm steel microparticle recorded in real time by high-speed camera are cropped from their initial size for the ease of comparison. The time stamps at the top of the frames indicate the delay in acquisition time relative to the first frame of the sequence. Rebound of microparticle from the material surface is evidenced in a) with a speed of 170 m/s and with minimum penetration as well as in b) with a speed of 77 m/s and a maximum DOP of about a full microparticle diameter.

In this type of analysis, we first consider the coefficient of restitution (COR), defined as the ratio of rebound velocity to impact velocity, or the square root of the ratio of the corresponding kinetic energies. The choice of COR is widely used as an empirical parameter to measure the energy dissipation for collisional events involving rebound.[29–31] In Fig. 3a, reproduced from Hsieh et al.,[28] the CORs obtained for the steel and silica particle impacts on PUU 532-1000 are compared as a function of impact velocity. In an ideal case with a completely elastic target, the COR would be equal to 1, assuming completely elastic projectiles. Meanwhile, in the case of impact by high-impedance steel microparticles the resulting impact

can drive the target further away from the elastic regime, which results in much lower values of COR, as shown in Fig. 3a. It is noteworthy that as impact velocity reaches a threshold velocity (~500 m/s), complete penetration of steel microparticles occurs, and thereafter the corresponding COR values become zero. In the case of silica microparticle impacts, we do not observe such transition even as velocities are increased up to 800 m/s.

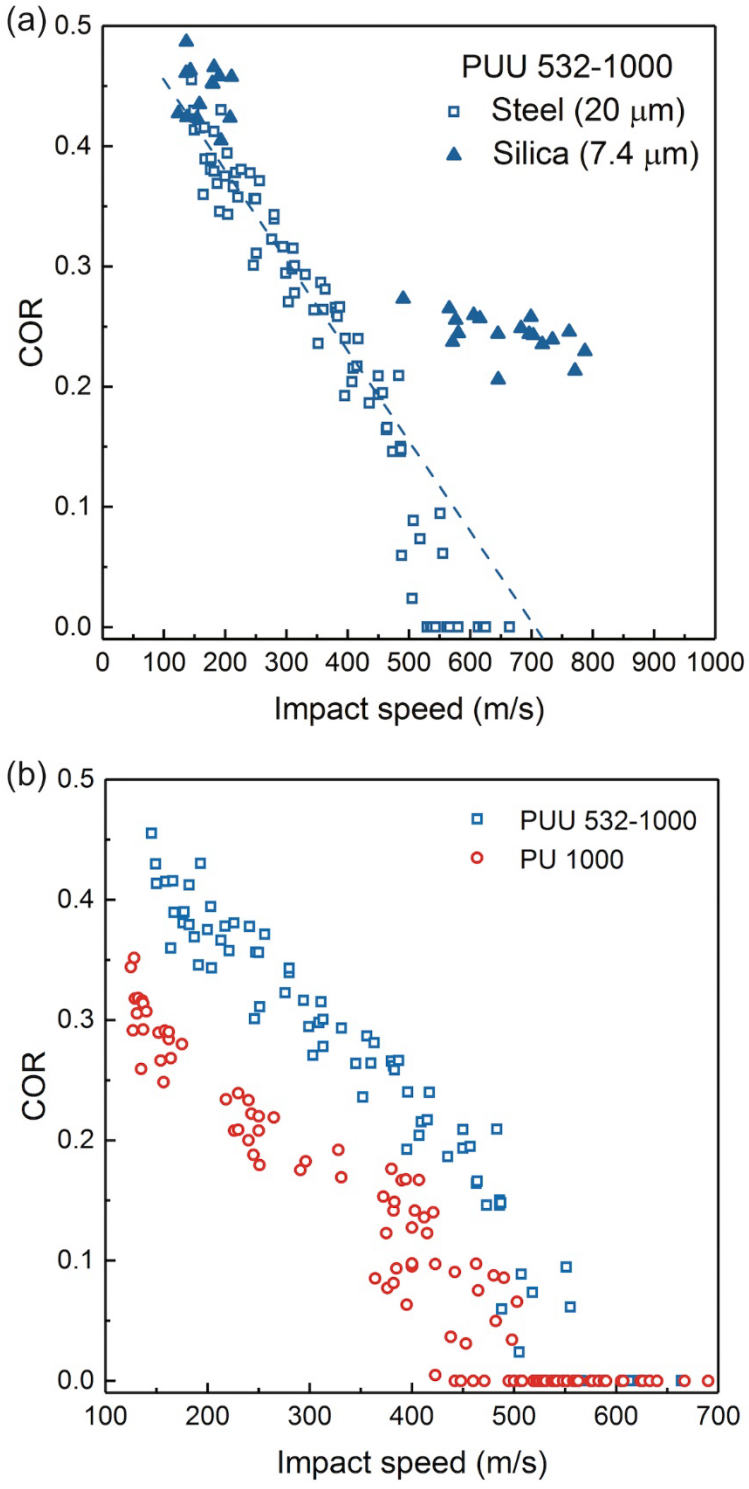

Fig. 3 a) Comparison of COR vs. impact speed determined for PUU 532-1000 upon impact via 7.4-μm silica particles and 20-μm steel particles (reproduced from Hsieh et al.[28]). The dashed line represents a linear fit of the data at low speed, 100–400 m/s, evidencing a sudden drop in the COR at around 500 m/s. b) Comparison of COR data for PUU 532-1000 and polyurea 1000 impacted with steel microparticles.

For comparison, microballistic impact measurements with steel projectiles were also carried out on polyurea 1000. In Fig. 3b, reproduced from Hsieh et al.,[28] the COR data obtained for the steel particles impacts on PUU 532-1000 and polyurea 1000 as a function of impact velocity are compared. As impact speed increases, a sudden drop in the COR occurs at around 475 and 400 m/s for PUU 532-1000 and polyurea 1000, respectively. It is noteworthy that PUU 532-1000 exhibits higher COR over the select impact velocity range as well as higher threshold velocity toward penetration than polyurea 1000. The compositional influence on the rate-dependent COR is consistent with the corresponding trend observed in the DOP measurements as shown in Fig. 4, reproduced from Hsieh et al.[28] A moderate improvement in the resistance against penetration, including both the normalized maximum depth and residual depth data, particularly at higher impact speeds, is noted for PUU 532-1000 (Fig. 4a) over polyurea 1000 (Fig. 4b). These observations are strongly indicative of greater dynamic stiffening and strengthening characteristics in PUU 532-1000 than the latter elastomer.

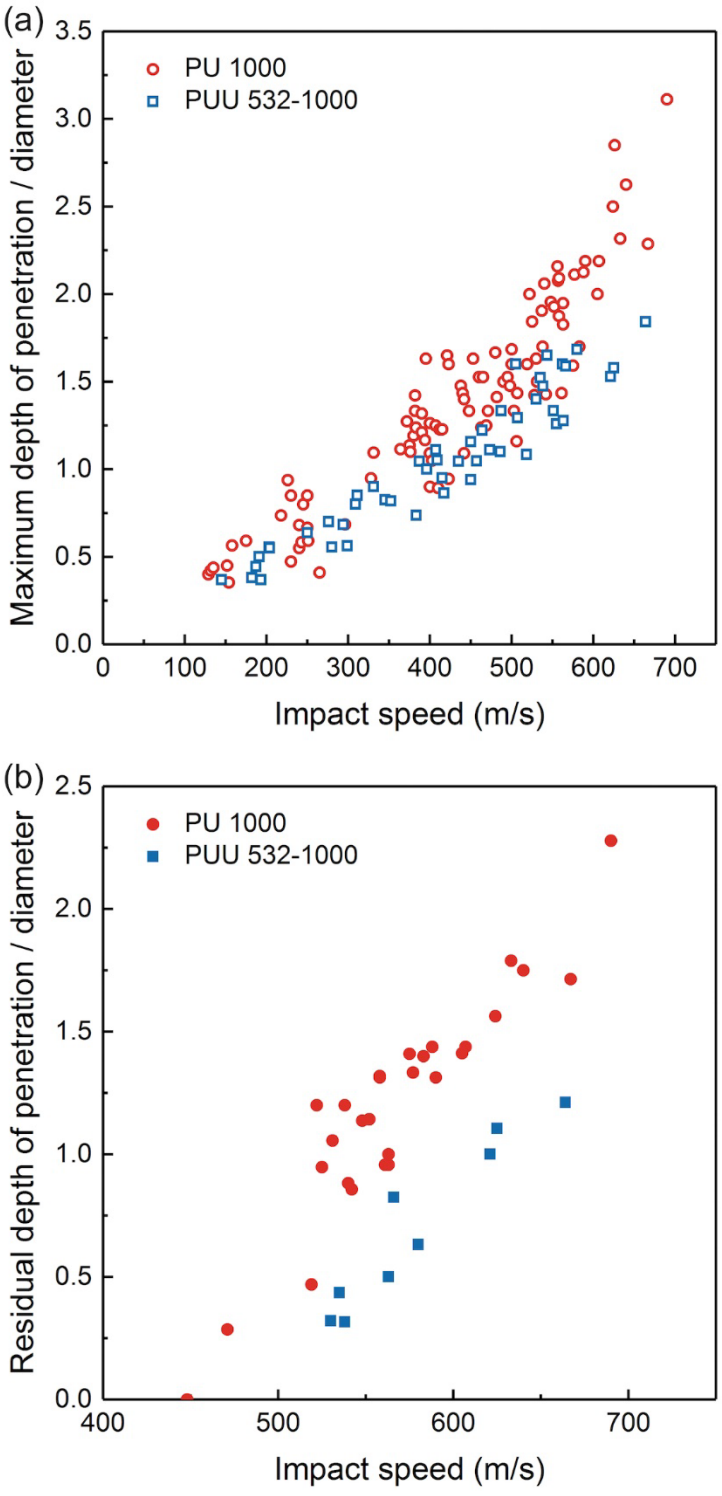

Fig. 4 Comparison of DOP data, including both the normalized maximum depth and normalized residual depth measurements after impact by steel microparticles, obtained for a) PUU 532-1000 and b) polyurea 1000 as a function of impact speed (reproduced from Hsieh et al.[28])

3.2 Molecular Influence on Segmental Relaxation

We investigated the molecular attributes that are of relevance toward dynamic stiffening and strengthening observed upon microballistic impact of the PUU 532-1000 and polyurea 1000 elastomers. Specifically, we focused on the role of segmental relaxations that are associated with the soft phase of each of the materials and the shift of these relaxations with respect to an increase in frequency, which are determined via broadband dielectric relaxation spectroscopy.

In this work, the broadband dielectric relaxation data are expressed in terms of a derivative form, by taking the logarithmic derivative of the dielectric constant, which has been shown with the same features as the loss spectra but without the DC conduction losses that often obscure low-frequency relaxation processes.[32,33] In Fig. 5a, reproduced from Hsieh et al.,[28] the isochronal dielectric loss data obtained for both PUU 532-1000 and polyurea 1000 at 1 Hz are compared. Correspondingly, Fig. 5b, reproduced from Hsieh et al.,[28] reveals the comparion of the dielectric data at 25 °C as a function of frequency. Distinct segmental α and local glassy state β relaxations are clearly evidenced in the PUU 532-1000 data, as shown in Fig. 5b, whereas a very broad ($\alpha_1 + \alpha_2$) process for polyurea 1000 is observed, in keeping with previous experimental findings.[24,34,35] Both segmental α relaxations are associated with the soft segments in the soft phases of these materials. In Fig. 5, a decrease in the dielectric loss is noted in PUU 532-1000 as compared with polyurea 1000. This is presumably the result of greater intersegment mixing in the soft phase of PUU 532-1000 since the PTMO soft segment molecular weight in each polymer is essentially the same and the corresponding hard segment contents are also similar. In comparison, a decrease in the dielectric loss was also observed as a result of a decrease in the molecular weight of PTMO[34] or an increase in the weight percent of hard segment.[35] This trend is consistent with in the compostion and microstructure dependence of the mechanical relaxation strength observed in dynamic mechanical analysis (DMA).[25,34] In addition, the influence of intersegment mixing is most clearly seen in Fig 5b in the much lower α relaxation frequency of PUU 532-1000 and in the indicated T_g's, –12 °C versus –36 °C for PUU 532-1000 and polyurea 1000, respectively, as shown in Fig. 6 (from performing a fit to the Vogel–Fulcher–Tamman [VFT] temperature dependence of the cooperative α process and extrapolating to τ_α=100 s), reproduced from Hsieh et al..[28] These observations are strongly indicative of the presence of soft phase with much slower segmental dynamics in PUU 532-1000 than in polyurea 1000.

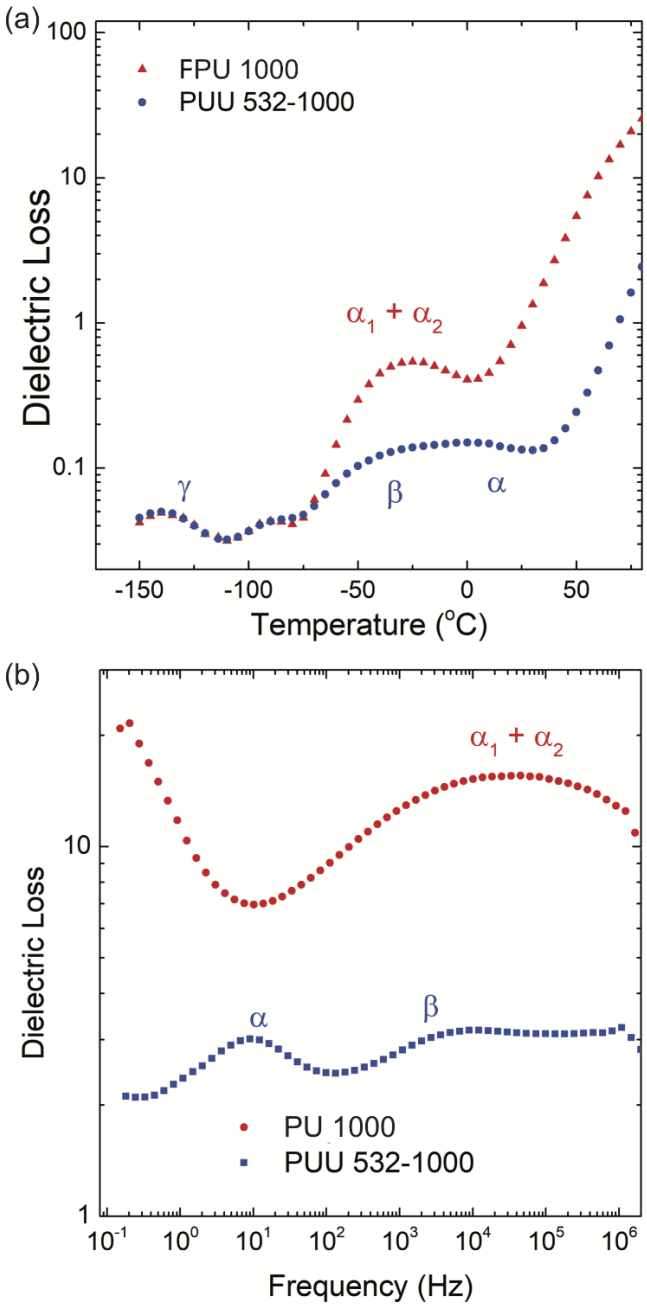

Fig. 5 Comparison of broadband dielectric relaxation data obtained for PUU 532-1000 and polyurea 1000 (reproduced from Hsieh et al.[28]): a) isochronal dielectric loss at 1 Hz as a function of temperature and b) dielectric loss at 25 °C as a function of frequency

To highlight the molecular influence, we compared the relaxation frequency maxima versus the reciprocal temperature data, as shown in Fig. 6, reproduced from Hsieh et al.[28] For both PUU 532-1000 and polyurea 1000, the respective segmental α relaxation reveals the expected VFT temperature dependence nature. Additionally, the segmental relaxation time, τ, was calculated following:

$\tau = 1/(2\pi f_{max})$, where f_{max} is the frequency of the maximum in the dielectric loss at each temperature.[36] For PUU 532-1000, the τ value of the phase-mixed soft phase at 25 °C is approximately 1.1×10^{-1} s, which is about four orders of magnitude slower than that of the broad segmental α relaxation of polyurea 1000, approximately 2.2×10^{-5} s. Such differences clearly elucidate that at ambient conditions the PUU 532-1000 would more easily undergo a high-rate deformation-induced glass transition than polyurea 1000 even when impacted at strain rates on the temporal scale of microseconds. Additionally, for PUU 532-1000 the segmental dynamics of the local β relaxation appears to be very close to that of the segmental α relaxation of polyurea 1000, indirectly suggesting that the extent of intersegment mixing in polyurea 1000 is significantly less than that in PUU 532-1000. This difference in the segmental relaxations observed between PUU 532-1000 and polyurea 1000 is further manifested based by the fact that their repective γ relaxations, which are presumably associated with the localized crankshaft motion of the ether oxygen-containing groups in the PTMO soft segments,[11,35,37] essentially overlap.

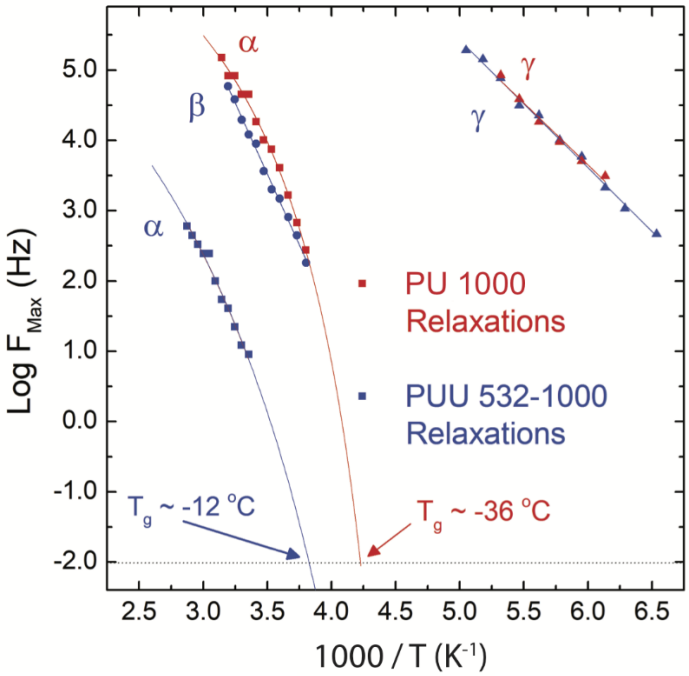

Fig. 6 Comparison of broadband dielectric relaxation data, logf_{max} vs. 1000/temperature, obtained for PUU 532-1000 and polyurea 1000, where solid lines are curve-fits of segmental α relaxations to a respective VFT equation, as well as of β and γ relaxations to a respective Arrhenius equation.[37] T_g's at τ_α = 100 s were determined to be –12 °C and –36 °C, respectively (reproduced from Hsieh et al.[28]).

Based on these broadband dielectric relaxation data, we expect that PUU532-1000 as well as polyurea 1000 would undergo high-rate deformation-induced glass

transition upon microballistic impact at strain rates on the order of 10^8/s. Meanwhile, PUU 532-1000, having a soft phase with much slower dynamics, would exhibit greater dynamic stiffening, which corroborates very well with the microballistic impact response—higher COR over the select impact velocity range, lower average normalized residual DOP, as well as higher threshold velocity toward penetration, than polyurea 1000, as shown in Figs. 3 and 4.

4. Discussion

4.1 Molecular Influence on Shock Hugoniot

The influence of molecular moieties was reported to be increasingly important as impulses become shorter.[38] For the bulk elastomers both PUU 532-1000[39] and polyurea 1000[40] exhibited similar shock Hugoniot data, as shown in Fig. 7, reproduced from Hsieh et al.[28] Meanwhile, one of the fundamental aspects of shock loading during plate impact is called impedance matching. If two surfaces maintain in contact during impact, the resulting particle velocity, u_p, and stress are presumably the same on both sides of the impact interfaces.[41] Details of plate impact measurements for PUU 532-1000 and polyurea 1000 can be found in Casem and Hsieh[39] and Mock et al.,[40] respectively. While PTMO soft segments have the same molecular weight in both polymers, we hypothesize that the presence of strong intermolecular hydrogen bonding in both polymers could also be plausible attributes to the similar shock Hugoniot. For comparison, the shock velocity data obtained for PUU 532-1000[39] and polyurea 1000[40] over the reported impact velocity range are very similar, as shown in Table 1.[28]

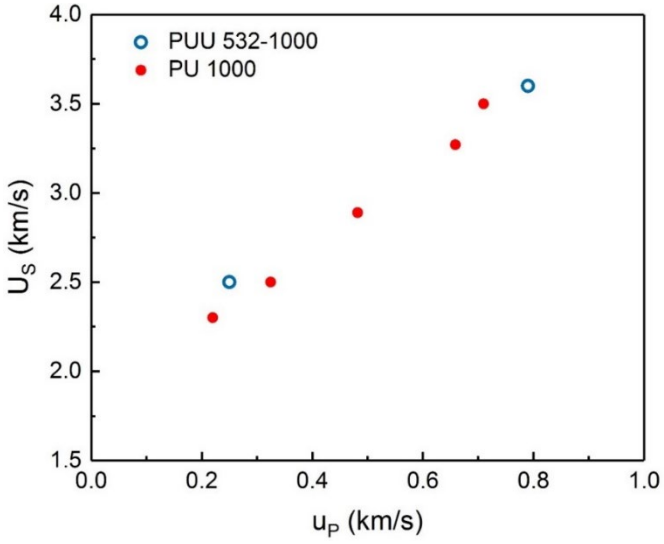

Fig. 7 Plot of Hugoniot U_s vs. u_p data for PUU 532-1000 (open blue circle)[39] and polyurea 1000 (solid red circle)[40] are included for comparison (reproduced from Hsieh et al.[28])

Table 1 Shock Hugoniot data reported for PUU 532-1000[39] and polyurea 1000[40]

Elastomer	Impact velocity (m/s)	Shock velocity U_s (km/s)	Particle velocity u_p (km/s)
PUU 532-1000	298	2.5	0.25
	998	3.6	0.79
Polyurea 1000	279	2.3	0.22
	921	3.5	0.71

4.2 Shock Wave Propagation at the Interface of a Glass/Polymer Bilayer Construct

Meanwhile, the nature associated with the refraction phenomenon of a stress wave propagating from one medium to another is known to be complex.[21,22] Here, for simplicity, we consider a 1-D steady-state shock wave that reaches the interface between materials of different shock impedance, Z, where the extent of energy that is reflected and transmitted at the interface is known to be dependent upon the difference in Z.[21] The greater the mismatch in Z, the greater the extent of energy will be reflected at the interface. In the case of a weak shock event, the fraction of the incident wave intensity that is reflected can be calculated with the equation[21]

$$\boldsymbol{R} = \left(\frac{\boldsymbol{Z_2 - Z_1}}{\boldsymbol{Z_2 + Z_1}}\right)^{\boldsymbol{2}}, \tag{1}$$

where Z_1 and Z_2 are the respective impedance of the materials.

For illustration, we consider the material response at the interface of a glass/PUU bilayer. For PUU 532-1000, the shock impedance (density × shock velocity) was calculated based on an extrapolation of the available shock velocity U_s data in Table 1.[28] Similarly for glass it was calculated based on the reported shock Hugoniot data in Carter and Marsh,[42] as shown in Table 2.[28] As u_p increases, the shock impedance for glass is 10.8 versus 3.2 MPa-s/m for PUU 532-1000 at 0.5 km/s, compared with the respective 11.1 versus 6.6 MPa-s/m at 2 km/s. This is strongly indicative of dynamic stiffening in PUU 532-1000, in spite of having much lower acoustic impedance than glass. Correspondingly, the extent of reflection, R, is reduced from 0.29 to 0.07, which is greatly desired, as it would presumably result in a significant reduction in the extent of tensile stress waves reflected from the back surface of glass. As a result, this would significantly mitigate the propensity toward crack propagation in the glass. Since both elastomers exhibit similar shock velocity data, we envision that polyurea 1000 is expected to behave very similarly

to PUU 532-1000 with respect to dynamic impedance optimization with glass, at the interface of a bilayer construct, particularly at the moment of impulse interaction.

Table 2 Shock velocity U_s and shock impedance Z calculated as a function of particle velocity for PUU, glass, and polycarbonate (PC)

u_p (km/s)		0.5	1	1.5	2
U_s (km/s)	PUU[b]	3.0	4.1	5.1	6.2
	Glass[c]	4.8	4.9	4.9	5.0
	PC[c]	3.2	3.9	4.7	5.4
Z[a] (MPa s/m)	PUU	3.2	4.3	5.5	6.6
	Glass	10.8	10.9	11.0	11.1
	PC	3.8	4.7	5.6	6.5

[a] Density (kg/m^3) data: 1061 for PUU 532-1000, as well as 2230 for glass,[42] and 1193 for bisphenol A. polycarbonate or PC[42]
[b] U_s vs. u_p data calculated based on the shock Hugoniot data[39]
[c] U_s vs. u_p data calculated based on the shock Hugoniot data[42]

To highlight the essence of segmental dynamics on dynamic impedance optimization, we compared PUU 532-1000 with glassy bisphenol A polycarbonate. The shock impedance data of PUU 532-1000 are very comparable to those of bisphenol A polycarbonate (Table 2[28]). This is in great contrast to their difference in the corresponding quasi-static properties, such as ambient storage modulus determined via DMA, which is approximately 0.3 GPa for PUU 532-1000 and much lower than that of polycarbonate, approximately 1.9 GPa.[11] Thus, unlike metals and glasses, the molecular influence including the enabling high-rate deformation-induced rubber-to-glass transition mechanism can be key to affecting the shock impedance of hierarchical elastomers.

4.3 Influence of Microstructure-Mediated Segmental Dynamics on High-Strain-Rate Impact Response

In addition to considering the shock-wave propagation at the interface, the underlying molecular attributes toward dynamic stiffening and strengthening of polymers can be critical to the overall ballistic impact performance of a glass/polymer bilayer. Specifically, we examine the role of segmental dynamics affecting the extent of hyperelastic response observed between these hierarchical elastomers upon impact at strain rates on the order of 10^8 s^{-1}. For illustration, we compare the extent of DOP data obtained from the microballistic measurements (Fig. 4a and Fig. 4b) at impact velocities, resulting in similar COR values for PUU 532-1000 and polyurea 1000. In the case of a COR of 0.25 ± 0.025 (highlighted in Fig. 8, reproduced from Hsieh et al.[28]), the respective impact speed was determined to be approximately 360 ± 60 m/s and approximately 190 ± 60 m/s for PUU 532-1000 and polyurea 1000, followed by the corresponding normalized DOP of

0.9 ± 0.2 (Fig. 9, reproduced from Hsieh et al.[28]) versus 0.7 ± 0.2 (Fig. 10, reproduced from Hsieh et al.[28]). These observations reveal that PUU 532-1000 is moderately more hyperelastic than polyurea 1000 upon microballistic measurements. This is consistent with the aforementioned resistance to penetration data, as shown in Fig. 4, where PUU 532-1000 exhibits moderate improvement in the normalized residual DOP over polyurea 1000.

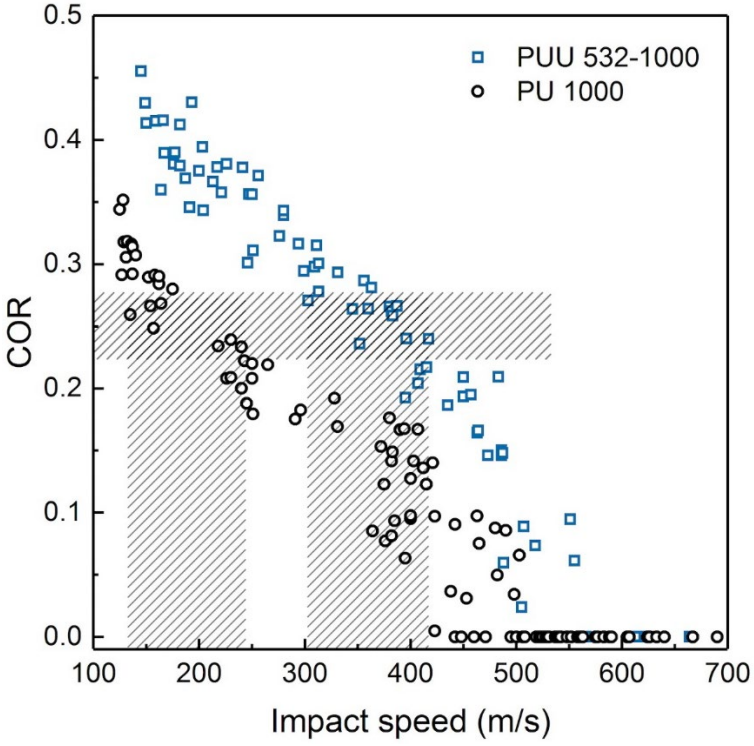

Fig. 8 a) Comparison of COR vs. impact speed determined for PUU 532-1000 upon impact via 20-μm steel microparticles. At a selected COR of 0.25 ± 0.025, the respective impact speed range was determined for PUU 532-1000 and polyurea 1000, as shown in the shaded area (reproduced from Hsieh et al.[28]).

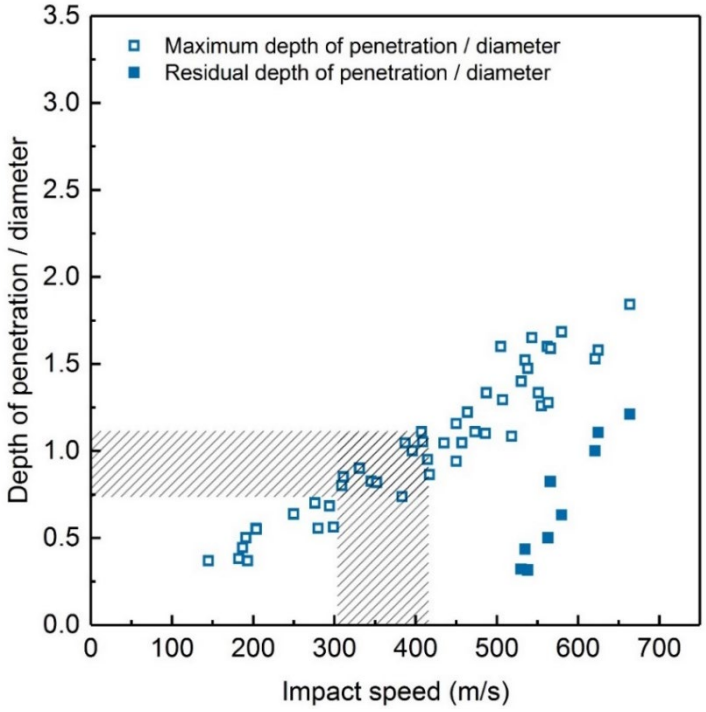

Fig. 9 Determination of maximum DOP obtained for PUU 532-1000 after impact via steel microparticles over a select impact speed range, highlighted by the shaded area (reproduced from Hsieh et al.[28])

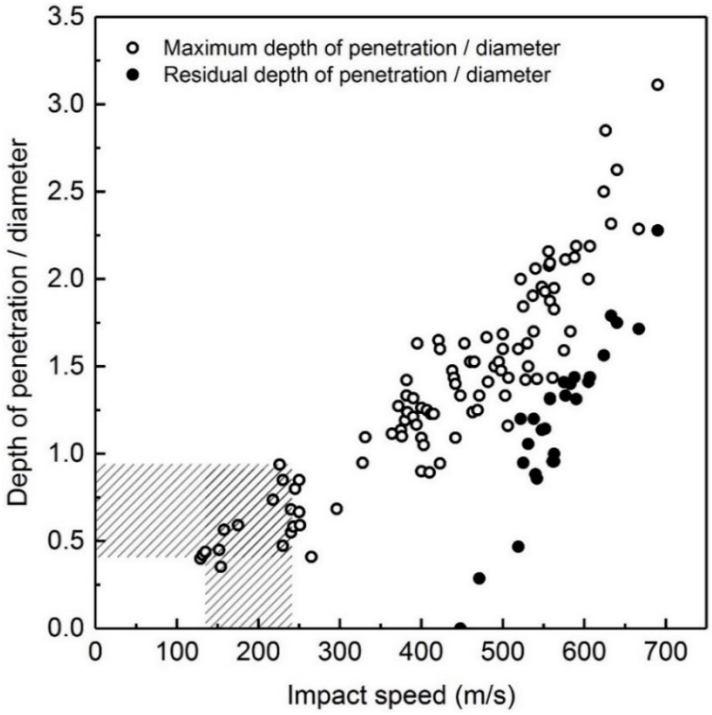

Fig. 10 Determination of maximum DOP obtained for polyurea 1000 after impact via steel microparticles over a select impact speed range, highlighted by the shaded area (reproduced from Hsieh et al.[28])

Furthermore, we highlight the influence of microstructure-mediated segmental dynamics on dynamic stiffening. For PUU 532-1000, the molecular mobility associated with the β relaxation at ambient temperature is expected to become significantly restricted as the frequency reaches approximately 10^4 Hz and above, as shown in Fig. 6. Thus, for PUU 532-1000, this local relaxation process would exhibit dynamic stiffening upon microballistic impact at strain rates of approximately 10^8/s. For PUU 532-1000 a shift of the β relaxation temperature to a higher temperature is noted in comparison with that of PUU 211-1000 (not shown). This could be due to the fact that PUUs were synthesized following a prepolymer route and increasing the molar ratio of the urea versus urethane linkages, from 1:1 for PUU 211-1000 to 1.5 for PUU 532-1000, which could presumably facilitate the ether oxygen containing linkages of soft segments with greater access toward intermolecular hydrogen bonding with ureas. As a result, it is envisioned that a cooperative molecular relaxation that couples soft segments through both segmental α and the local β relaxations could be a plausible pathway for PUU 532-1000 toward dynamic stiffening and strengthening upon impact over the temporal scale of microseconds to nanoseconds.

Although little is known regarding the composition and microstructure of commercially available polyurethane elastomers, we hypothesize that the presence of intermolecular hydrogen bonding readily available in polyurethanes like in PUU and polyurea elastomers could facilitate a cooperative relaxation throughout an interconnected hydrogen-bonded polymer network. This serves as a motivation toward future studies via exploiting atomistic molecular dynamic simulations to further discern and differentiate molecular attributes, including both molecular conformations and intermolecular bonding strength that are of relevance to the dynamic pressure compressibility upon ballistic shock interaction. This would lead to better understanding of molecular mechanisms as well as provide guidance toward design and synthesis of advanced interlayer materials for use in high-performance laminated glass/polymer composites to achieve enhanced ballistic impact protection capability.

5. Conclusion

The influence of interlayer elastomers, particularly the role of segmental dynamics, which could affect the ballistic shock response at the interface of a glass/polymer bilayer, particularly at the moment of impulse/target interaction, was investigated.

First, we elucidated the dynamic stiffening characteristics that were observed in PUU elastomers upon microballistic impact by silica microparticles, which was also evidenced during impact with steel microparticles at strain rates of

approximately 10^8/s. Rebound of steel microparticles also occurred when PUU 532-1000 was impacted at speeds below approximately 500 m/s. Additionally, PUU 532-1000 exhibited higher COR over the select impact velocity range, as well as higher threshold velocity toward penetration, than polyurea 1000. The composition influence on the rate-dependent COR is consistent with the corresponding trend observed in the resistance against penetration data. A moderate improvement was noted in the normalized residual DOP data, particularly at higher impact speeds, for PUU 532-1000 in comparison with polyurea 1000. These are strongly indicative of greater dynamic stiffening and strengthening of PUU 532-1000 than polyurea 1000. The molecular influence on the extent of dynamic stiffening response corroborated well with the prediction based on the segmental dynamics data determined via broadband dielectric relaxation spectroscopy. PUU 532-1000 exhibits greater intersegment mixing than polyurea 1000, and as a result the dynamic glass transition temperatures determined at τ_α = 100 s are –12 °C versus –36 °C, respectively. For PUU 532-1000, the segmental α relaxation assocaited with the soft phase having gretaer intersegment mixing was determined to be about four orders of magnitude slower than that of the broad segmental α relaxation of polyurea 1000. Additionally, the segmental dynamics of the local β relaxation of PUU 532-1000 appeared to be very close to that of the segmental α relaxation of polyurea 1000, which further indirectly suggests greater intersegment mixing in PUU 532-1000 than the latter. We hypothesize that the presence of strong intermolecular hydrogen bonding along with PTMO of 1000-g/mol molecular weight in both elastomers could be the plausible attributes for the similar shock Hugoniot data. As a result, it is envisioned that polyurea 1000 will behave very similarly to PUU 532-1000 when considering the dynamic impedance optimization with glass, at the interface of a bilayer construct, particularly at the moment of impulse interaction. Meanwhile, PUU 532-1000 is prone to greater dynamic stiffening than polyurea 1000 upon impact over the temporal scale of microseconds to nanoseconds, presumably due to the presence of well-coupled segmental α and local β relaxations in PUU.

Based on these observations, we hypothesize that a high-rate deformation-induced glass-transition mechanism could be a plausible pathway toward dynamic stiffening of interlayer elastomers, which would otherwise not be realized based on material properties from manufacturers. This is critical, as it could also enable dynamic impedance optimization at the interface between glass and a polymer sublayer during ballistic impact, particularly at the moment of impulse/target interaction. Meanwhile, through the analysis of shock-wave propagation we calculated the extent of shock wave reflection that would occur at the interface of a glass/polymer bilayer, where dynamic shock impedance was calculated from

shock velocity, which was derived from the shock Hugoniot of the respective materials. As it was shown, a significant reduction in the extent of reflection can be achieved at the interface of a glass/PUU bilayer, which is greatly desired, as it would presumably mitigate the extent of tensile stress waves reflected from the interface back into the glass and correspondingly the propensity toward further fracture in the glass.

While hierarchical elastomers with multiple relaxations on the temporal scale from microseconds to nanoseconds are desired for dynamic impedance optimization with glass, it is also envisioned that a new design paradigm based on a bilayer adhesive-interlayers concept could be of benefit for incorporation into the design of next generation laminated glass/polymer composites. In a bilayer adhesive construct, the interlayer next to glass is designed with greater dynamic stiffening capability predominantly for dynamic shock impedance optimization with glass. Meanwhile, the inner adhesive layer can enable desired dynamic strengthening characteristics as well as adequate adhesion for bonding with the subsequent polymer layers.

6. References

1. McCauley JW. Lightweight protective materials: ceramics, polymers, and metals. In: Opportunities in Protection Materials Science and Technology for Future Army Applications. Washington (DC): The National Academies Press; 2011.

2. Sands JM, Patel PJ, Dehmer PG, Hsieh AJ, Boyce MC. Protecting the future force: transparent materials safeguard the Army's vision. The AMPTIAC Quarterly. 2004;8(4):28–36.

3. Gupta YM, Ding JL. Impact load spreading in layered materials and structures: concept and quantitative measure. International Journal of Impact Engineering. 2002;27:277–291.

4. Patel PJ, Hsieh AJ, Gilde GA. Improved low-cost multi-hit transparent armor. Presented at the 25th Army Science Conference; 2006 Nov 27–30; Orlando, FL.

5. Espinosa HD, Rim JE, Barthelat F, Buehler MJ. Merger of structure and material in nacre and bone – perspectives on de novo biomimetic materials. Progress in Materials Science. 2009;54:1059–1100.

6. Wegst UGK, Bai H, Saiz E, Tomsia AP, Ritchie RO. Bioinspired structural materials. Nature Materials. 2015;14(1):23–36.

7. Chen Y, Wang L. Bio-inspired heterogeneous composites for broadband vibration mitigation. Sci Rep. 2015;5:17865.

8. Huang J, Durden H, Chowdhury M. Bio-inspired armor protective material systems for ballistic shock mitigation. Materials and Design. 2011;32(7):3702–3710.

9. Meyers MA, Chen P-Y, Lin A.Y-M, Seki Y. Biological materials: structure and mechanical properties. Prog in Mat Sci. 2008;53(1):1–206.

10. Veysset D, Hsieh AJ, Kooi SE, Maznev AA, Masser KA, Nelson KA. Dynamics of supersonic microparticle impact on elastomers revealed by real-time multi-frame imaging. Sci Rep. 2016;6:25577.

11. Veysset D, Hsieh AJ, Kooi SE, Nelson KA. Molecular influence in high-strain-rate microparticle impact response of poly(urethane urea) elastomers. Polymer. 2017;123:30–38.

12. Hassani-Gangaraj M, Veysset D, Nelson KA, Schuh CA. In-situ observations of single micro-particle impact bonding. Scr Mater. 2018;145:9–13.

13. Hassani-Gangaraj M, Veysset D, Nelson KA, Schuh CA. Melting can hinder impact-induced adhesion. Phys Rev Lett. 2017;119:175701.

14. Wang CB, Cooper SL. Morphology and properties of segmented polyether polyurethaneureas. Macromolecules. 1983;16:775–786.

15. Sheth JP, Aneja A, Wilkes GL, Yilgor E, Atilla GE, Yilgor I, Beyer FL. Influence of system variables on the morphological and dynamic mechanical behavior of polydimethylsiloxane based segmented polyurethane and polyurea copolymers: a comparative perspective. Polymer. 2004;45:6919–6932.

16. Strawhecker KE, Hsieh AJ, Chantawansri TL, Kalcioglu ZI, Van Vliet KJ, Influence of microstructure on micro-/nano-mechanical measurements of select model transparent poly(urethane urea) elastomers. Polymer. 2013;54:901–908.

17. Hsieh AJ, Chantawansri TL, Hu W, Strawhecker KE, Casem DT, Eliason JK, Nelson KA, Parsons EM. New insight into microstructure-mediated segmental dynamics in select model poly(urethane urea) elastomers. Polymer. 2014;55:1883–1892.

18. Hu W, Hsieh AJ. Phase-mixing and molecular dynamics in poly(urethane urea) elastomers by solid-state NMR. Polymer. 2013;54:6218.

19. Hsieh AJ, Chantawansri TL, Hu W, Cain J, Yu JH. New insight into the influence of molecular dynamics of matrix elastomers on ballistic impact deformation in UHMWPE composites. Polymer. 2016;95:52–61.

20. Meyers MA. Dynamic behavior of materials. Hoboken (NJ): John Wiley and Sons, Inc; 1994.

21. Henderson LF. On the refraction of shock waves. J Fluid Mech. 1989;198:365–386.

22. Kanel GI, Razorenov NV, Fortov VE. The failure waves and spallations in homogeneous brittle materials. In: Schmidt SC, Dick RD, Forbes JW, Tasker DG, editors. Proceedings of the American Physical Society Topical Conference, Shock Compression of Condensed Matter; 1991; Williamsburg, VA.

23. Sarva SS, Hsieh AJ. The effect of microstructure on the rate-dependent stress-strain behavior of poly(urethane urea) elastomers. Polymer. 2009;50(13):3007–3015.

24. Choi T, Fragiadakis D, Roland CM, Runt J. Microstructure and segmental dynamics of polyurea under uniaxial deformation. Macromolecules. 2012;45:3581−3589.

25. Rinaldi RG, Hsieh AJ, Boyce MC. Tunable microstructures and mechanical deformation in transparent poly(urethane urea)s. J Polym Sci Part B Polym Phys. 2011;49:123–135.

26. Fragiadakis D, Gamache R, Bogoslovov RB, Roland CM. Segmental dynamics of polyurea: effect of stoichiometry. Polymer. 2010;51:178–184.

27. Lee J-H, Veysset D, Singer JP, Retsch M, Saini G, Pezeril T, Nelson KA, Thomas EL. High strain rate deformation of layered nanocomposites. Nat Commun. 2012;3:1164.

28. Hsieh AJ, Veysset D, Miranda DF, Kooi SE, Runt J, Nelson KA. Polymer, molecular influence in the glass/polymer interface design: the role of segmental dynamics. 2018;146:222–229.

29. Calvit HH. Experiments on rebound of steel balls from blocks of polymer. J Mech Phys Solids. 1967;15:141–150.

30. Constantinides G, Tweedie CA, Holbrook DM, Barragan P, Smith JF, Van Vliet KJ. Quantifying deformation and energy dissipation of polymeric surfaces under localized impact. Mater Sci Eng A. 2008;489:403–412.

31. Diani J, Gilormini P, Agbobada G. Experimental study and numerical simulation of the vertical bounce of a polymer ball over a wide temperature range. J Mater Sci. 2014;49:2154–63.

32. Wubbenhorst M, van Turnhout J. Analysis of complex dielectric spectra. I. One-dimensional derivative techniques and three-dimensional modeling. J Non-Crys Solids. 2002;305(1-3):40–49.

33. van Turnhout J, Wubbenhorst M. Analysis of complex dielectric spectra. II: Evaluation of the activation energy landscape by differential sampling. J Non-Cryst Solids. 2002;305(1-3):50–58.

34. Castagna AM, Pangon A, Choi T, Dillon GP, Runt J. The role of soft segment molecular weight on microphase separation and dynamics of bulk polymerized polyureas. Macromolecules. 2012;45:8438–8444.

35. Castagna AM, Fragiadakis D, Lee H-K, Choi T, Runt J. The role of hard segment content on the molecular dynamics of poly(tetramethylene oxide)-based polyurethane copolymers. Macromolecules. 2011;44:7831–7836.

36. Roland CM, Casalini R. Effect of hydrostatic pressure on the viscoelastic response of polyuria. Polymer. 2007;48:5747–5752.

37. Fragiadakis D, Runt J. Macromolecules, molecular dynamics of segmented polyurethane copolymers: influence of soft segment composition. 2013;46:4184–4190.

38. Bourne NK. On the shock response of polymers to extreme loading. J Dyn Behav Mater. 2016;2:33–42.

39. Casem DT, Hsieh AJ. Plate-impact measurements of a select model poly(urethane urea) elastomer. Aberdeen Proving Ground (MD): Army Research Laboratory (US); 2013 Aug. Report No.: ARL-TR-6482.

40. Mock W Jr, Bartyczak S, Lee G, Fedderly J, Jordan K. Dynamic properties of polyurea 1000. American Institute of Physics Conference Proceedings. 2009;1195(1):1241–1244.

41. Proud WG. Notes on shock compression, wave propagation and spall strength. London (UK): Institute of Shock Physics, Imperial College. http://www.mta.ro/wp-content/uploads/2015/12/Proud_William_GSEBS__ImperialCollege_2015_-4.pdf

42. Carter W, Marsh S. Hugoniot equation of state of polymers. Los Alamos (NM): Los Alamos National Laboratory; 1985. Report No.: LA-13006-MS.

List of Symbols, Abbreviations, and Acronyms

1-D	1-dimensional
ARL	US Army Research Laboratory
COR	coefficient of restitution
DETA	diethyltoluenediamine
DMA	dynamic mechanical analysis
DOP	depth of penetration
HMDI	4,4'-dicyclohexylmethane diisocyanate
ONR	Office of Naval Research
PTMO	poly(tetramethylene oxide)
PUU	poly(urethane urea)
VFT	Vogel–Fulcher–Tamman
Z	shock impedance

1 (PDF) DEFENSE TECHNICAL INFORMATION CTR DTIC OCA

2 (PDF) DIR ARL
IMAL HRA
RECORDS MGMT
RDRL DCL
TECH LIB

1 (PDF) GOVT PRINTG OFC
A MALHOTRA

4 (PDF) ARL
RDRL WM
AM RAWLETT
RDRL WMM
CF YEN
RDRL WMM E
PJ PATEL
RDRL WMM G
AJ HSIEH